Fiber Optic Sensor System for Defect Classification using Novel Physics based Modelling and Data Driven Approach

Anish Gorantiwar
Center for Tire Research (CenTiRe)
Virginia Tech
anishg@vt.edu

Rajvardhan Nalawade
Center for Tire Research (CenTiRe)
Virginia Tech
rajvardhan@vt.edu

Arash Nouri
Center for Tire Research (CenTiRe)
Virginia Tech
anouri@vt.edu

Vahid Sotoudeh
EXIR Principal
vahidsmail-exir@yahoo.com

Behzad Moslehi
Intelligent Fiber Optic Systems Corporation (IFOS)
bm@ifos.com

William Price
Intelligent Fiber Optic Systems Corporation (IFOS)
wp@ifos.com

Feraidoon Zahiri
Robins AFB, GA, USA
feraidoon.zahiri@us.af.mil

Saied Taheri
Center for Tire Research (CenTiRe)
Virginia Tech
staheri@vt.edu

Abstract—**This paper discusses a new framework for Machine Health Diagnosis in the field of Structural Health Monitoring. A physics-based approach has been combined with a data-driven methodology to classify structural defects using vibration data from Fiber Bragg Grating (FBG) sensors. Three system architectures were developed comprising physics-based modeling, feature extraction via different data processing techniques and end-to-end defect classification algorithms for an in-house built bearing test-rig. A test rig consisting of a bearing-motor-shaft assembly was developed in-house for data generation and for real-time implementation of the defect detection and classification algorithms. In order to place the sensors in the right locations, a simplified Finite Element (FE) Model of the test rig was developed. Using the data from this FE model, the FBG sensors were installed on the test rig. Data processing algorithms were developed in time as well as frequency domains to extract features from the vibration data collected using these sensors. This includes developing Wavelet algorithms to generate two-dimensional spectral energy data. These features were then used with a developed Convolutional Neural Network (CNN) model which outputs the classification labels corresponding to the different types of bearing defects and defect intensities. Based on the algorithm evaluation, accuracies of 98% and 98.9% were achieved for bearing defect detection and defect intensity, respectively. As a next step, these algorithms will be implemented in an additive manufacturing environment to detect and classify part defects as they are being built.**

TABLE OF CONTENTS

978-1-6654-3760-8/22/$31.00 ©2022 IEEE

1. INTRODUCTION

Condition based maintenance (CBM) is a maintenance strategy which essentially suggests maintenance decisions based on the information collected through health monitoring. This information is collected through an array of sensors both exteroceptive - which give information of the surrounding relative to machine body and proprioceptive - which give information regarding the machine itself.

Two important aspects of CBM lie in defect classification and Remaining Useful Life (RUL) estimation which essentially corresponds to structural health monitoring and machine prognosis [1]. In this paper, emphasis has been given on developing a framework for defect classification for a rotary bearing based test rig. Rolling element bearings play a crucial role in various mechanical engineering assemblies ranging from small gearboxes to heavy industrial equipment. A defect in any portion of the bearing may result in the overall breakdown of the machine and hence it is of prime importance to detect these defects early during the machine operation. In order to sense these vibration signals, different sensors can be used, the selection of which depends upon various parameters such as frequency range, resolution and the required sensitivity amongst others.

In [2], piezoelectric based accelerometers along with a load cell have been used for bearing defect classification via time and frequency domain features. To overcome the inherent frequency range limitation of accelerometers, Fiber Bragg

Gratings (FBG's) have just being started to use for condition health monitoring.

In [3], a review consisting of an experimental setup comprising of a network of FBG sensors for temperature and strain monitoring is discussed. The sensors also provide information on the loading and traffic status of the passenger cars, temperature-induced stresses and deformations on rails and carriages, dynamic axle vibrations due to corrosion and bearing wear, and other parameters relevant to rail road health monitoring. A key outcome of this work is that the FBG sensors can easily capture high frequency dynamic strains.

For defect classification, different approaches have been considered which make use of time, frequency and time-frequency domain features, to extract meaningful information from the vibration data ([4], [5], [6]).

Researchers in [7] extracted time domain based statistical features from the vibration signals and trained multi-class Support vector Machines (SVM's) to classify between the different bearing defects. In accordance with this, [8] developed Artificial Neural Networks (ANN's) combined with genetic algorithms to select the most significant input parameters from a larger set of input features for bearing defect monitoring.

In [9], statistical features from time and frequency domains were used in combination with Hilbert transforms to get a feature matrix and further using Principal Component Analysis (PCA) for dimensionality reduction. This approach extended further from the previous work wherein features from both domains were used and a Fuzzy C-means clustering method to determine the classification efficacy.

In a study [10], degradation signals considered focused on the evolution of the Root Mean Square (RMS) vibration level over time. This information was then used to train neural network models on predicting bearing operating times. The proposed methodology in [11] uses time domain features extracted from vibration signals as health indicators. The degradation states in bearings are detected by an unsupervised classification technique called artificial ant clustering. The imminence of the next degradation state in bearings is given by hidden Markov models, and the estimation of the remaining time before the next degradation state is given by the multi-step time series prediction and the adaptive neuro-fuzzy inference system.

Studies have also been conducted in using time-frequency domain based approach by utilizing wavelets for feature extraction. In [12], the authors show the use of complex wavelet analysis for feature extraction and further developing SVM and ANN for bearing defect classification. Research has also been carried out in defect identification in gears by using genetic algorithms for selecting the optimum mother wavelet and carrying out comparison studies between different wavelet types([13], [14], [15]).

Along with using standard machine algorithms, Convolutional Neural Networks (CNN's) have also been used to identify different types of bearing faults. Vibration data acquired from accelerometers have been stacked together to form 2-D matrices and then passed to different convolution and pooling layers. Use of scaled-Fourier Transforms and adaptive CNN's have also been developed for better feature extraction and classification([16], [17], [18], [19]).

Table 1. FEA Simulation Conditions

Property	Value
Shaft Material	Hardened Steel
Bearing Material	Chrome Steel
Mesh Size	2x2
Element Type	4-node iso-parametric quadrilateral strain

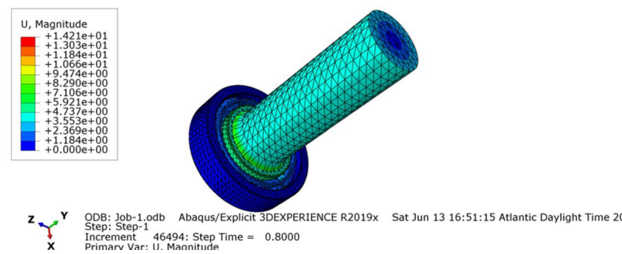

Figure 1. FEA - Normal Bearing Condition

In this paper, algorithms have been developed encompassing time, frequency and wavelet based signal processing techniques and using end-to-end machine learning models for bearing defect classification. In coordination with this, similar algorithms have been implemented for classifying between the different intensities of a single bearing defect.

This paper is structured as follows: Section (2) consists of the Finite Element Model (FEM) development, Section (3) contains information regarding the experimental test rig and the sensor subsystems, Section (4) comprises of the different data processing techniques, Section (5) consists of the machine learning model development and Section (6) includes the implementation of algorithm for defect intensity classification and Section (7) comprises of conclusions and future scope of the project.

2. FINITE ELEMENT ANALYSIS (FEA)

The first subsystem of the complete architecture comprises of developing a physics-based numerical model of the test-rig. This has been completed by developing a Finite Element Model (FEM) in Abaqus software.

A 3-dimensional FEA model has been constructed comprising of the test rig components - shaft, bearing inner race, bearing outer race and the intermediate ball bearings. The material properties and the simulation conditions have been enlisted in Table 1.

The FEA model consists of 3 different case scenarios - Normal Bearing, Inner Race Defect Bearing and Missing Ball Bearing. This has been done for analyzing the locations on the bearing which is most sensitive to defects and can capture their vibration characteristics. The FEA stress and displacement analysis for each of the following cases can be seen in Figures 1, 2 and 3, respectively.

Following this, Dynamic analysis was done in FEA by giving a predefined angular velocity to the bearing. The nodes on the outer casing on the Plummer block were observed for displacement (Figure 4) and velocity (Figure 5) characteristics in different operating conditions. With this, it was seen that the outer casing of bearing is a suitable location for observing

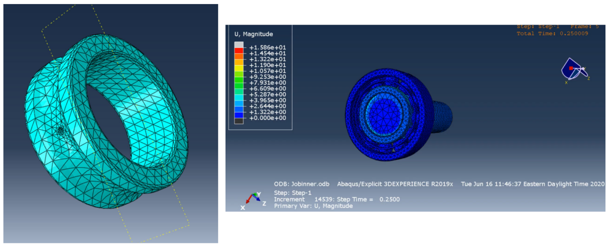

Figure 2. **FEA - Inner Race Bearing Defect**

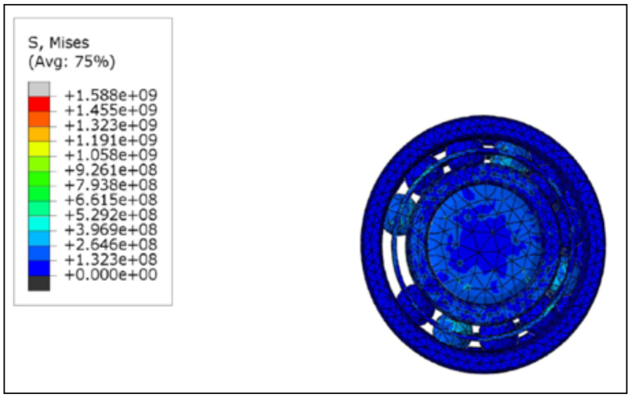

Figure 3. **FEA - Missing Ball Bearing Defect**

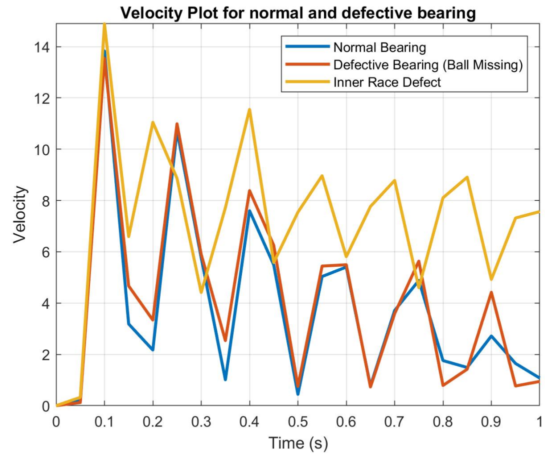

Figure 5. **Nodal Velocity for different bearing conditions**

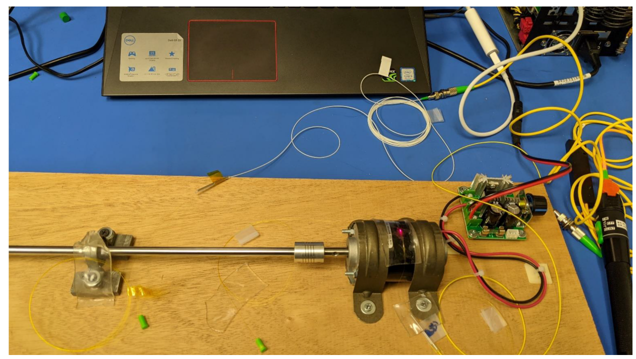

Figure 6. **Experimental Setup - Bearing Test Rig**

varying bearing vibration characteristics. In addition to this, the location was geometrically suitable to place a sensor and collect data easily. The study concluded with the identified sensor location being the outer race casing of the bearing for optimal signal sensing.

3. Experimental Setup

An experimental test rig has been developed consisting of a bearing-motor-controller assembly. The test rig can be seen in Figure 6. Different bearing defect cases were tested on this test rig and the data was collected via Fiber Bragg Grating (FBG) sensors and the corresponding data acquisition system. Based upon the FEA analysis, the plummer block of the bearing was decided as the optimal location for mounting the FBG sensor.

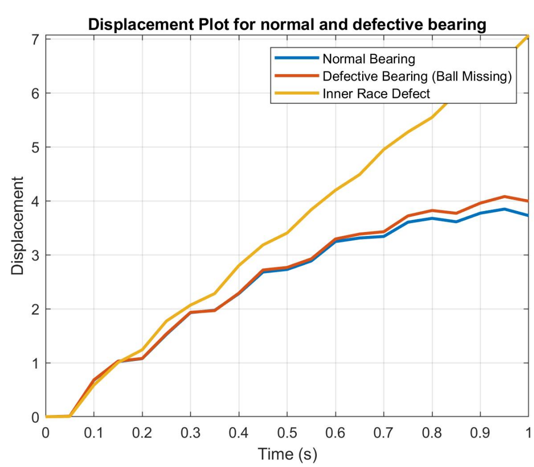

Figure 4. **Nodal Displacement for different bearing conditions**

The experimental setup consists of the components shown in Table 2.

FBG Sensor

The FBG sensor is essentially an optical fiber sensor that operates by acting as a wavelength selective optical filter that reflects an ultra narrow spectral band centered at a wavelength called as the Bragg wavelength. The spectral width defined by the passband of such a grating forms a channel that reflects the narrow slice of optical spectrum centered at the characteristic Bragg wavelength, allowing the remainder of the spectrum to pass through the fiber with negligible optical loss. The key advantages of using FBG sensors in this work have been listed below:

Table 2. **Experimental Setup Components**

Number	Component
1	FBG Sensor
2	FBG Interrogator
3	Plummer block ball bearing
4	DC Motor and Driver
5	Shaft and coupling pair
6	Variable DC Power Supply

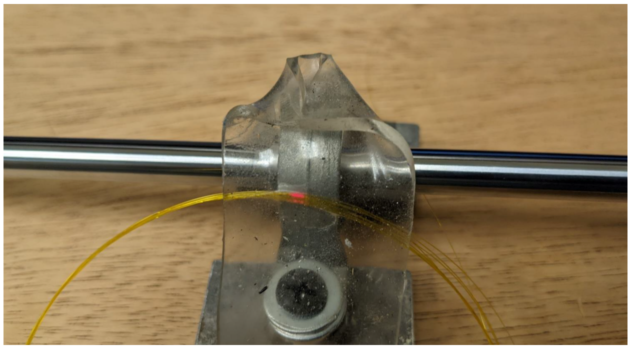

Figure 7. FBG Sensor mounted on bearing plummer block

- The wideband (from DC to at least hundreds of kHz) response of FBG's makes them excellent acoustic emissions detection sensors. This helps in capturing high and low frequency vibration characteristics.
- Compared to conventional PZT-based (Lead zirconium titanate) sensors, FBG's and the optical fiber in which they reside are extremely low mass and minimally thermally conductive, electrically passive, chemically inert, and highly multiplexable.

The FBG sensor used has a sampling rate of 1.3MHz and it was mounted on the plummer block of the bearing for data collection. Figure 7 shows the FBG sensor mounted on the plummer block of the bearing.

FBG Interrogator

The FBG interrogator is essentially a data acquisition system for collecting and analyzing the FBG data.

Plummer block ball bearing

A plummer/pillow block ball bearing has been used as the primary component for defect classification. The bearing consists of the following major components:

- Inner Race
- Outer Race
- Ball and Cage arrangement
- Plummer block

A bearing with an 8mm bore diameter has been selected with Zinc alloy being the inner and outer race material.

DC Motor and Driver

A 12V Permanent Magnet DC motor has used been used for driving the bearing mounted on the shaft. The motor has been controlled via speed controller to obtain data for different shaft rotational velocities ranging from 1000 - 2700 RPM.

Shaft and coupling pair

An 8mm solid aluminum shaft has been used for mounting the bearing. This shaft is connected to the motor shaft via a flexible coupling. The use of a flexible coupling over rigid flange coupling allows for taking into account geometrical central inaccuracies between the two shafts.

Testing Conditions

Data has been collected for two different testing scenarios for classifying both - different bearing defects and different intensities of a single bearing defect. The following subsections give a insight into the two different test scenarios:

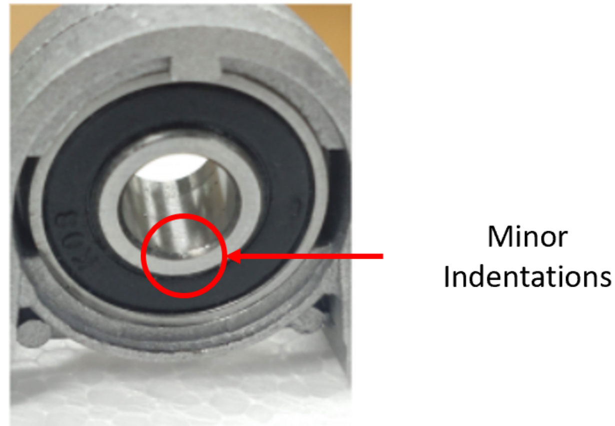

Figure 8. Bearing with Inner Race Defect

Bearing Defect Classification—Defects were induced in different components of the bearing as discussed in the previous subsection which corresponds to the common bearing failure regions. Defects, in the form of minor indentations, were induced to have the following 4 defect classes:

- Bearing Inner Race Defect
- Bearing Outer Race Defect
- Bearing Hybrid Defect - Corresponding to defects induced in both inner and outer race
- Normal Bearing

Figure 8 shows the indentations produced on the inner race of the bearing.

Bearing Defect Intensity Classification—Along with classifying different types of defects, the levels of intensity of a particular defect were also analyzed by progressively increasing the depth of the indentation/cut on the inner race of the bearing. Six different depth defects were developed on the inner race of the bearing which can be seen in Figure 9.

4. DATA PROCESSING

Three different data processing techniques have been applied on the FBG vibration data in order to extract relevant features which have been further used to develop and train the machine learning models for defect classification.

Figure 10 shows the time series plot of the different defect conditions of the bearing. From this Figure, we can see that each of the operating conditions have a different vibration signature. Along with this, the data has been further normalized to keep uniformity during analyzing and processing the data.,

The following subsections entail the working of all the three data processing techniques:

Time Domain

The vibration data corresponding to different bearing defects can be better analyzed by computing statistical features of this data which gives better insights in the data variations between these different defect types. These time domain statistical features along with their description have been listed in Table 3.

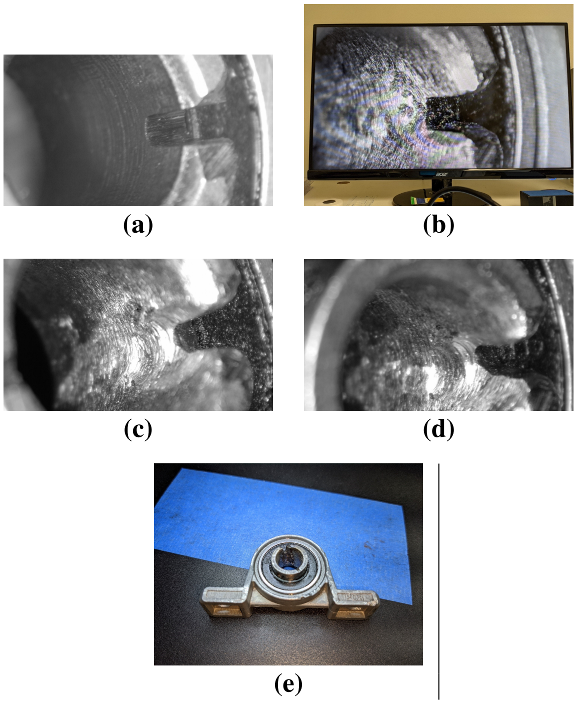

Figure 9. **(a)** First Cut **(b)** Third Cut **(c)** Fourth Cut **(d)** Fifth Cut **(e)** Sixth Cut

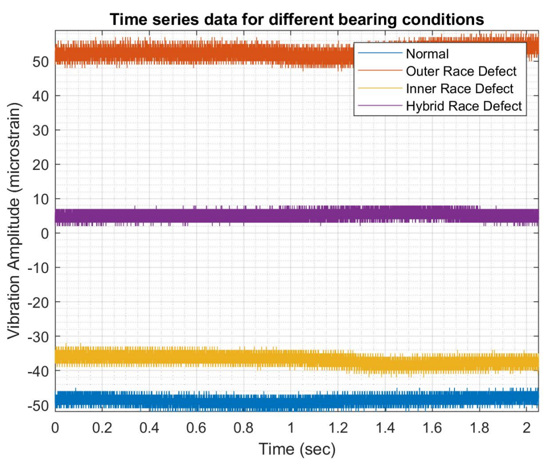

Figure 10. **Time Domain Raw Bearing Data for different bearing conditions**

The FBG raw data has been normalized to remove any bias in the data and has been converted to micro-strain values via a scaling factor. This data has been further sub-sampled into smaller batch sizes and the above statistical features have been computed for each of the batch sizes.

Figure 11 shows the variations of the statistical features for each of the bearing defect. Significant differences between these statistical features can be evaluated. These features have then been given as inputs to the classification algorithm for distinguishing between different bearing defect types.

Frequency Domain

The defects developed in different components of the bearing, as mentioned above, have their own characteristics frequency i.e., these defects tend to occur at the harmonics of this characteristic frequency.

Table 3. **Time Series Statistical Features**

Number	Component
Mean	Average value of vibration signal
Standard Deviation	Measure of signal deviation from mean value
Skewness	Measure of lack of symmetry in the signal
Kurtosis	Measure of whether the given distribution consists of extreme values
Root Mean Square (RMS)	Quadratic Mean of the signal
Crest Factor	Peak value divided by the RMS. Faults often first manifest themselves in changes in the peakiness of a signal before they manifest in the energy represented by the signal root mean squared.

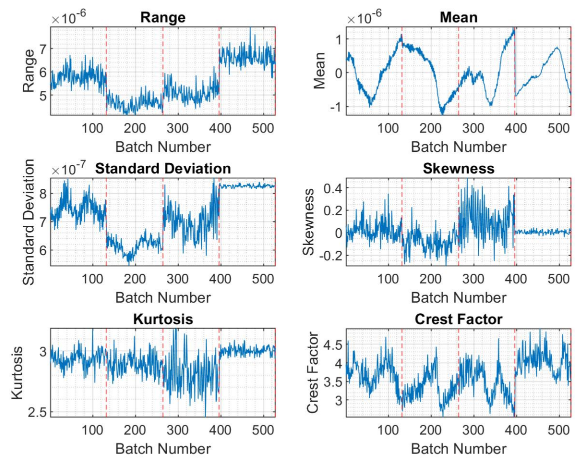

Figure 11. **Time Domain Statistical Features**

These frequency harmonics can be derived analytically and they depend on the geometrical properties of the bearing along with the shaft rotation speed. For defects developed in the outer race and inner race, two such frequencies exist, which are described below.

- BPFO (Ball Pass Frequency Outer): This frequency corresponds physically to the number of balls or rollers that pass through a given point of the outer race each time the shaft makes a complete rotation.

$$\mathbf{BPFO} = f_m * \frac{n}{2} * (1 - \frac{D}{d} * cos(\beta)) \quad (1)$$

- BPFI (Ball Pass Frequency Inner): This frequency corresponds physically to the number of balls or rollers that pass through a given point of the inner track each time the shaft makes a complete rotation.

$$\mathbf{BPFI} = f_m * \frac{n}{2} * (1 + \frac{D}{d} * cos(\beta)) \quad (2)$$

where

f_m = Shaft Rotation Speed
n = Number of balls
β = Contact Angle
D = Ball Diameter
d = Pitch Circle Diameter of the Bearing

Fast Fourier transform of the signal is calculated by using Welch's method to see the frequency domain characteristics of the FBG data. As the conversion of a signal from time domain to frequency domain is sensitive to effects of noise, it is necessary to have a method that would not be affected by the presence of stochastic noise in the signal. Hence, instead of extracting the Fourier coefficients of the time domain signal, Welch's method involving averaging and Hamming windowing is used. Equation 3 shows the Welch's equation.

$$w(n) = 0.54 - 0.46cos(2\pi\frac{n}{N}) \tag{3}$$

where,
$0 \leq n \leq N$
N is the total number of points
w are the coefficients of the Hamming window

The power spectrum values corresponding to the BPFO and BPFI harmonics have been extracted and have been fed as feature vectors to the machine learning algorithm for defect classification.

Time-Frequency Domain

The third approach for the defect classification lies in the time-frequency domain based analysis. As opposed to the previous approach, in which time domain signal were studied, having a spectral approach enables to gain useful insight on the information available in both the time-frequency and spatial space. A wavelet based approach is proposed over using Short Term Fourier Transforms (STFT) as the required window length can be changed by dilating and translating the wavelets, which provides the freedom to choose the time and frequency resolutions, respectively. The frequency resolution is better at lower frequencies and the time resolution is enhanced at high frequencies for a wavelet transform.

Based on an extensive literature review, continuous Morlet wavelet has been selected, having equal variance in both time and frequency domains, for defect classification.

An important reason for going with this approach is that the bearing failure, due to these defects, can be further classified based on different frequency bands. This helps in determining what type of failure occurs at what frequency level. These zones are listed as follows:

- Stage 1: Acoustic emission: During the bearing operation, bursts of acoustic emissions (AE) result from the passage of the defect through the roller and raceway contacts. Defects at different locations of a bearing (inner race, roller and outer race) have characteristic frequencies at which bursts are generated – above 100kHz. The data corresponding to these frequency ranges can identify subtle defects like lack of lubrication.
- Stage 2: Ultrasonic frequencies: In ball bearings, as the metal in the raceway, roller or ball elements begins to fatigue, a subtle deformation begins to occur. This deforming of the metal produces irregular surfaces, which cause an increase in the emission of ultrasonic sound waves (24 to 100kHz).

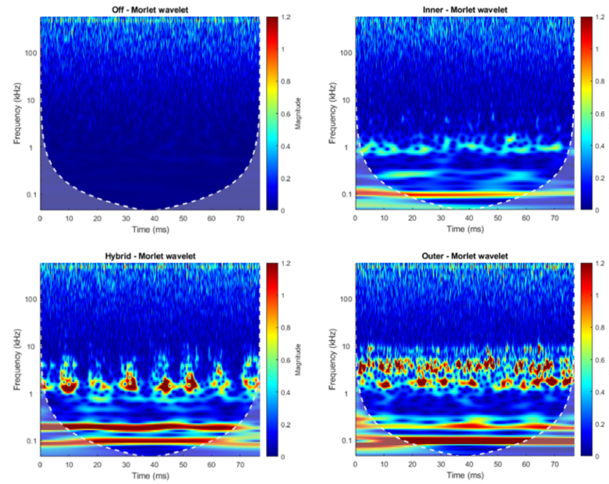

Figure 12. **Scalograms for different bearing defect types**

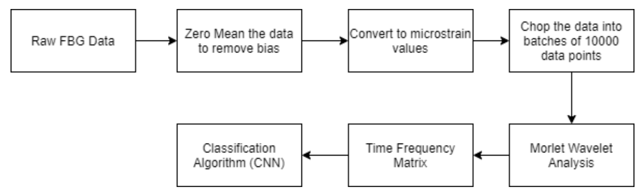

Figure 13. **Time-Frequency Methodology**

- Stage 3: Rotational harmonics: Defects start to ring at the bearing's natural frequencies. This generally occurs between 500 and 5,000 Hz. These natural frequencies may be resonances of either bearing support structures or components of the bearings themselves such as races or rolling elements. Side-band frequencies also start to appear above and below these frequencies.

Figure 12 shows the scalograms for different defect conditions of the bearing. From this Figure, we can see that, especially at lower frequencies, there is a substantial difference in the energy content between the different test conditions

The overall process followed for the time-frequency analysis can be seen in Figure 13. Initially the raw FBG data is normalized and converted to micro-strain values for better evaluation. The entire data is then sub-sampled into smaller batch sizes of 10000 data points each and the continuous Morlet wavelet transformation is performed for each of these batch sizes. The resulting time-frequency matrices was given as input to the machine learning based classification algorithm

5. Machine Learning Model Development

Based on the three different data processing techniques used, two classes of machine learning models have been developed:

- Physics Based: Multi-layered Perceptron (MLP) models have been developed which uses the time-domain based statistical features and the Power spectrum values in frequency domain as inputs and computes the classification metrics for the defect identification.
- An end-to-end deep CNN based classification model has been developed which takes the time-frequency matrix as

input and outputs the classification metrics.

Time Domain Classification Model

The statistical features extracted from the time domain signal have been fed to the MLP algorithm as input vectors and after extensive tuning of the hyper-parameters using the Grid Search Method, a testing classification accuracy of **86.84%** was obtained. The model architecture can be seen in Figure 14.

Furthermore, in order to analyze the classification performance, confusion matrix was plotted which can be seen in Figure 15. From this matrix we can see that the model makes the main diagonal has the maximum number of samples indicating that each class is correctly identified with less number of mis-classifications as is evident from the small number of non-diagonal samples.

Frequency Domain Classification Model

The Power Spectrum density (PSD) values corresponding to the BPFO and BPFI harmonics have been taken as inputs for the MLP classification algorithm and the performance of the model has been evaluated by analyzing the confusion matrix. The corresponding model architecture can be seen in Figure 16.

The confusion matrix for the frequency domain based classification can be seen in Figure 17. The classification accuracy improved slightly than the time domain based approach to **88.57%** indicating that the energy content at the harmonics of fault frequencies act as important features in bearing defect classification.

End-to-end Learning Framework

As discussed in Section 4, continuous Morlet wavelet has been used to generate spectral maps for the four defect classes which have been then fed as input tensors to a CNN architecture. Deep learning based CNN framework has been selected because by keeping the time-frequency image as a matrix, the spatial variation is preserved, which otherwise would have been lost by flattening the data.

The input feature is the time-frequency matrix, which is essentially a grayscale image, and the output is the condition of the bearing. In order to characterize the noise within the system, FBG data was also collected when the test rig was in an idle condition and this scenario has been treated as a separate class while performing the defect classification. Since there are 5 classes – Normal bearing, Inner race defect, outer race defect, hybrid defect, and static noise (bearing not running), this is a 5-class classification problem.

The architecture of the CNN model is described below:

- The input feature vectors are grayscale images of size 221x221.
- These feature images are then fed to a convolution layer with a 3x3 Gaussian kernel and 10 filters in each convolution layer.
- The activation function used is 'Rectified Linear Unit' due to its reduced likelihood of the gradient to vanish, being computationally efficient (as only 'max' operation needs to computed) and having better convergence performance.
- The resulting feature map is then fed to a Max pooling layer to generate a feature map containing the most prominent features of the previous feature map.
- This has been repeated for three convolution layers fol-

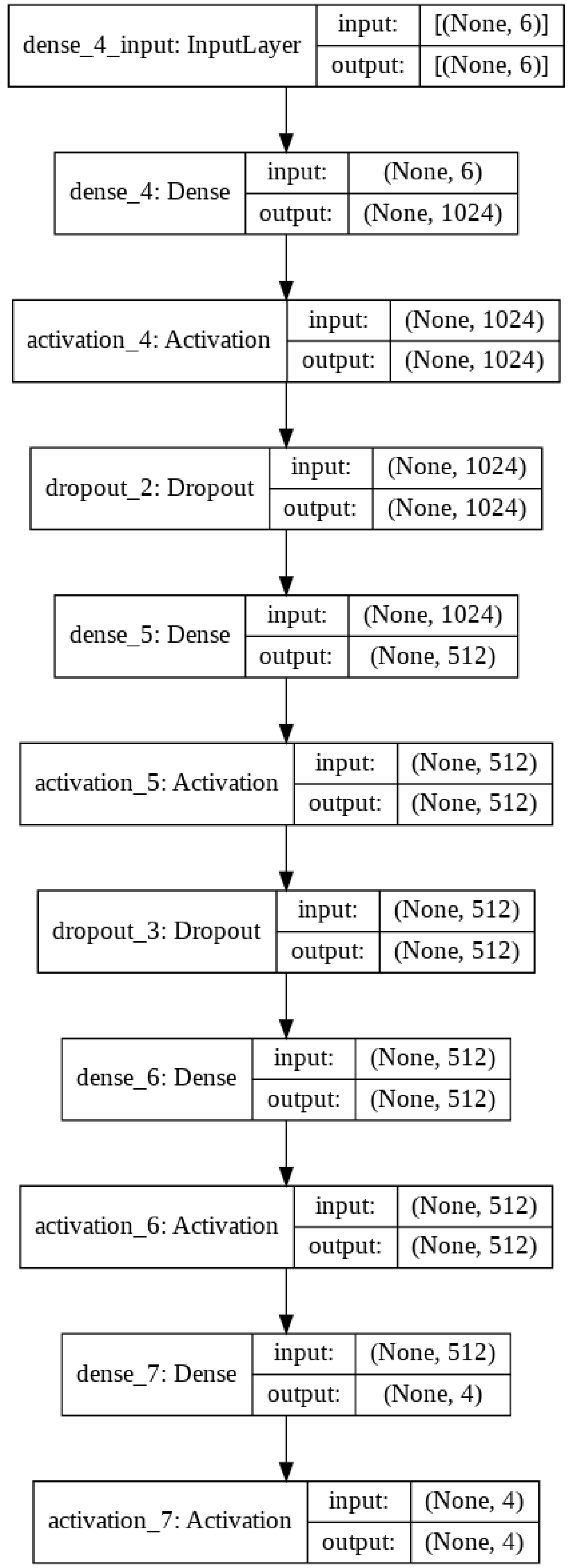

Figure 14. Time domain based MLP architecture

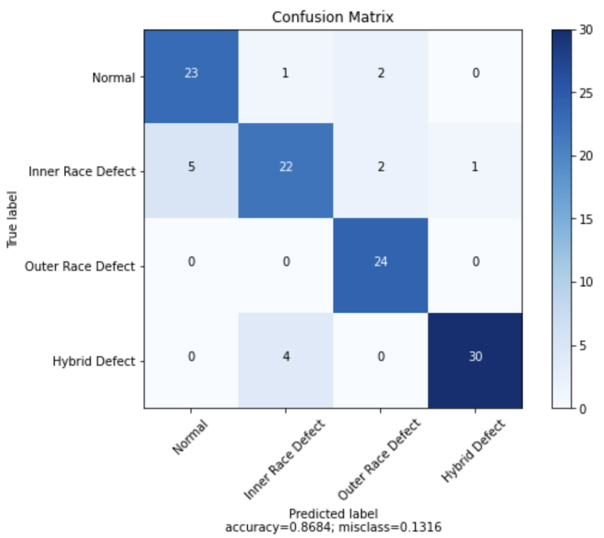

Figure 15. Confusion Matrix - Time Domain

lowed by a flatten layer and fully connected dense layers to make classifications.

A Key point to notice is that the entire time-frequency matrix is given to the CNN architecture in the form of an image input. In this way, the model can focus on all 3 frequency zones and can identify the slight damages in a bearing. This also makes the approach very scalable. CNN's help preserve the spatial variation of time and frequency data. The input image can be transformed into various domains, by multiplying with kernels, and better features can be extracted. The model automatically understands which frequencies to focus on, corresponding to the severity of defect in bearing.

Figure 18 shows the confusion matrix and the corresponding precision and recall scores for the 5-class classification algorithm. A classification accuracy of **98%** was obtained using this approach. This is significantly higher than the previous two approaches indicating that the wavelet based approach, due to its ability of focusing on all frequency ranges, gives a higher classification performance.

6. Defect Intensity Classification

Based on an in-depth analysis of the three defect classification algorithms developed, it can be seen that the time-frequency based approach has the highest values of classification performance metrics. A key reason for this is that the physics based models of time and frequency domain do not necessarily capture the non-linear effects created by the defects in the bearing. Hence, the same framework has also been used to characterize an inner race bearing defect of varying intensity and classify between these intensities of defect.

Figure 19 shows the time series plot of the six different intensities of the inner race defect discussed in Section 3. Levels 1-6 indicate progressively higher intensities of the defect.

A wavelet process similar to that for classifying the different defect types has been followed. Figure 20 shows the scalograms for the 6 levels of the intensity of the defect. From this Figure, it can be seen that as the defect size increases, the energy content increases in the lower frequency ranges.

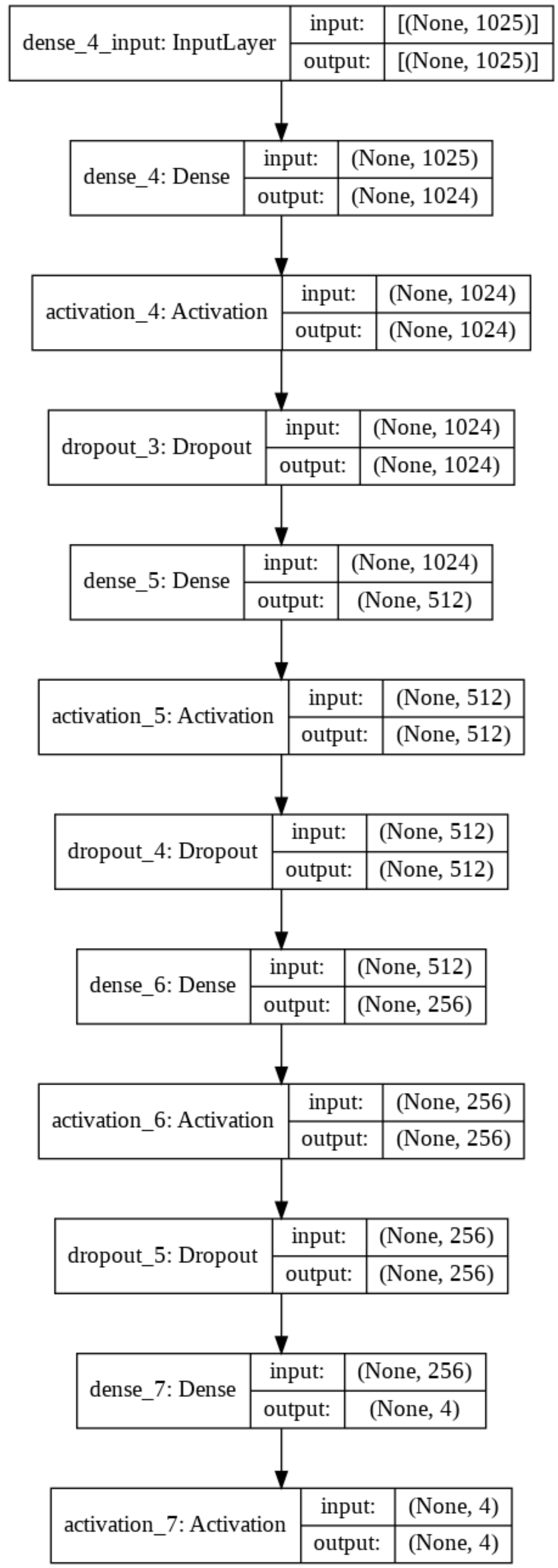

Figure 16. Frequency domain based MLP architecture

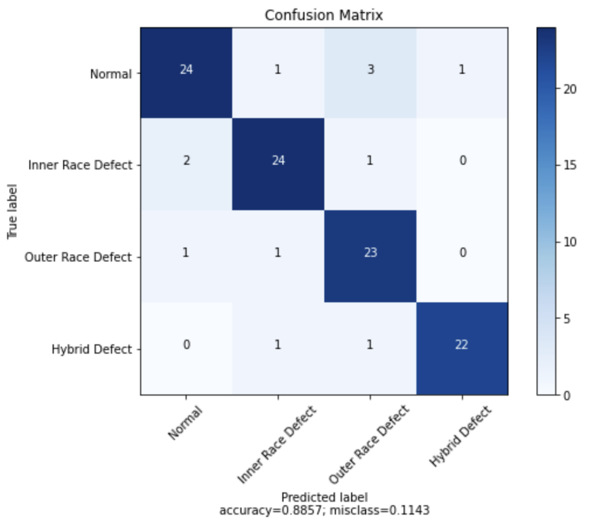

Figure 17. Confusion Matrix - Frequency Domain

	precision	recall	f1-score	support
hybrid	1.00	0.98	0.99	50
normal	0.96	0.96	0.96	50
outer	1.00	1.00	1.00	50
inner	0.96	0.98	0.97	50
noise	1.00	1.00	1.00	50
accuracy			0.98	250
macro avg	0.98	0.98	0.98	250
weighted avg	0.98	0.98	0.98	250

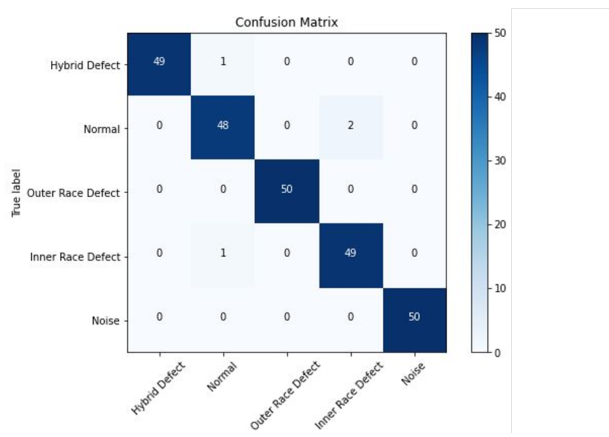

Figure 18. Confusion Matrix - Time Frequency Domain - Bearing Defect Type

The CNN algorithm developed for classifying the bearing defect types has been re-implemented for defect intensity classification. Figure 21 shows the confusion matrix for intensity classification along with the corresponding precision, recall and F1-scores for the different damage levels. A classification accuracy of **98.9%** has been obtained for defect intensity classification using this approach.

7. Conclusions and Future Work

In this paper, a framework has been developed for classifying different bearing defect types and different intensities of bearing defects. A three system architecture has been implemented comprising of first developing a physics based Finite Element Model for identifying potential sensor locations on the test rig to collect meaningful vibration data. Second, three different data processing techniques have been developed in time, frequency and time-frequency domains to extract key feature vectors from this FBG data. Third, end-to-end machine learning model has been developed for classifying different bearing defect types. Based on the evaluation of each of these models, it has been found that the time-frequency based approach has the highest classification performance metrics and hence this model has further been used to classify between defects of varying intensity.

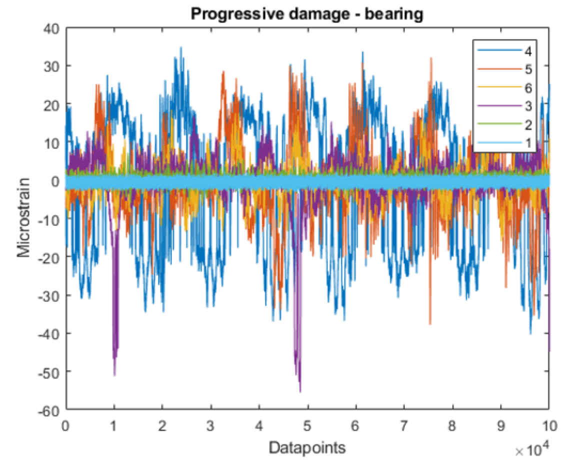

Figure 19. Varying Defect Intensity Time Series Plot

The next steps in this research consist of extending this framework in identifying potential defects in 3D printed products while they are being additively manufactured and locating the corresponding defects within the part structure.

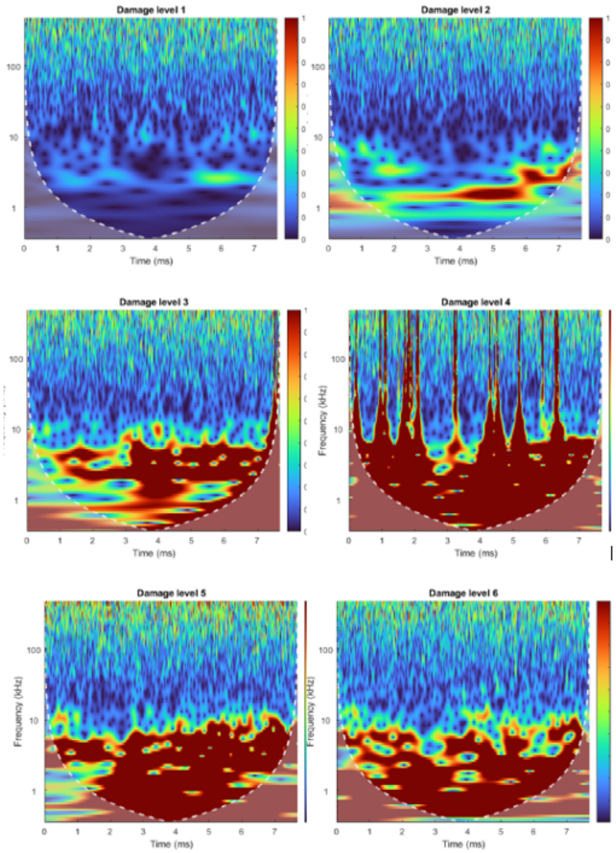

Figure 20. **Scalograms for varying defect intensity**

	precision	recall	f1-score	support
dam1	1.00	0.96	0.98	50
dam2	1.00	1.00	1.00	50
dam3	0.96	0.98	0.97	50
dam4	0.98	1.00	0.99	50
dam5	1.00	1.00	1.00	50
dam6	1.00	1.00	1.00	50
accuracy			0.99	300
macro avg	0.99	0.99	0.99	300
weighted avg	0.99	0.99	0.99	300

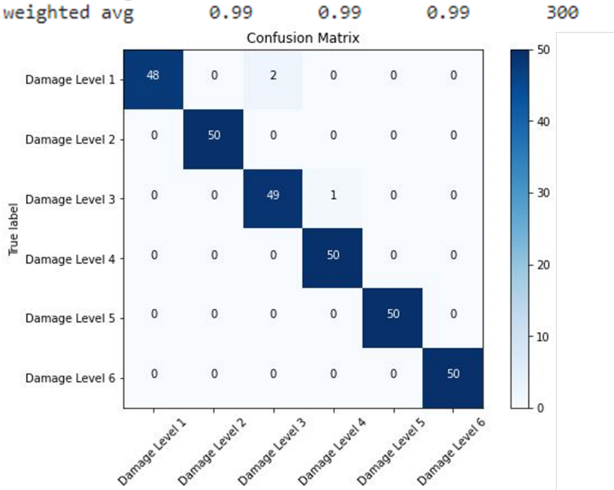

Figure 21. **Confusion Matrix - Time Frequency Domain - Defect Intensity**

References

[1] M. Saxena, O. O. Bannett, and V. Sharma, "Bearing fault evaluation for structural health monitoring, fault detection, failure prevention and prognosis," *Procedia Engineering*, vol. 144, pp. 208–214, 2016.

[2] M. Safizadeh and S. Latifi, "Using multi-sensor data fusion for vibration fault diagnosis of rolling element bearings by accelerometer and load cell," *Information fusion*, vol. 18, pp. 1–8, 2014.

[3] H. Y. Tam, T. Lee, S. Ho, T. Haber, T. Graver, and A. Méndez, "Utilization of fiber optic bragg grating sensing systems for health monitoring in railway applications," *Structural Health Monitoring*, vol. 2, pp. 1824–1831, 2007.

[4] F. Bonnardot, R. Randall, J. Antoni, and F. Guillet, "Enhanced unsupervised noise cancellation using angular resampling for planetary bearing fault diagnosis," *International journal of acoustics and vibration*, vol. 9, no. 2, pp. 51–60, 2004.

[5] A. Sharma, M. Amarnath, and P. Kankar, "Feature extraction and fault severity classification in ball bearings," *Journal of Vibration and Control*, vol. 22, no. 1, pp. 176–192, 2016.

[6] J. Wang, L. Cui, H. Wang, and P. Chen, "Improved complexity based on time-frequency analysis in bearing quantitative diagnosis," *Advances in Mechanical Engineering*, vol. 5, p. 258506, 2013.

[7] O. R. Seryasat, F. Honarvar, A. Rahmani, *et al.*, "Multi-fault diagnosis of ball bearing based on features extracted from time-domain and multi-class support vector machine (msvm)," in *2010 IEEE International Conference on Systems, Man and Cybernetics*, pp. 4300–4303, IEEE, 2010.

[8] L. Jack and A. Nandi, "Genetic algorithms for feature selection in machine condition monitoring with vibration signals," *IEE Proceedings-Vision, Image and Signal Processing*, vol. 147, no. 3, pp. 205–212, 2000.

[9] F. Wang, J. Sun, D. Yan, S. Zhang, L. Cui, and Y. Xu, "A feature extraction method for fault classification of rolling bearing based on pca," in *Journal of Physics: Conference Series*, vol. 628, p. 012079, IOP Publishing, 2015.

[10] N. Gebraeel, M. Lawley, R. Liu, and V. Parmeshwaran, "Residual life predictions from vibration-based degradation signals: a neural network approach," *IEEE Transactions on industrial electronics*, vol. 51, no. 3, pp. 694–700, 2004.

[11] A. Soualhi, H. Razik, G. Clerc, and D. D. Doan, "Prognosis of bearing failures using hidden markov models and the adaptive neuro-fuzzy inference system," *IEEE Transactions on Industrial Electronics*, vol. 61, no. 6, pp. 2864–2874, 2013.

[12] C. Malla, A. Rai, V. Kaul, and I. Panigrahi, "Rolling element bearing fault detection based on the complex morlet wavelet transform and performance evaluation using artificial neural network and support vector machine," *Noise & Vibration Worldwide*, vol. 50, no. 9-11, pp. 313–327, 2019.

[13] J. Rafiee, P. Tse, A. Harifi, and M. Sadeghi, "A novel technique for selecting mother wavelet function using an intelli gent fault diagnosis system," *Expert Systems with Applications*, vol. 36, no. 3, pp. 4862–4875, 2009.

[14] K. Feng, Z. Jiang, W. He, and Q. Qin, "Rolling element bearing fault detection based on optimal antisymmetric real laplace wavelet," *Measurement*, vol. 44, no. 9, pp. 1582–1591, 2011.

[15] L. Tóth and T. Tóth, "On finding better wavelet basis for bearing fault detection," *Acta Polytechnica Hungarica*, vol. 10, no. 3, pp. 17–35, 2013.

[16] O. Janssens, V. Slavkovikj, B. Vervisch, K. Stockman, M. Loccufier, S. Verstockt, R. Van de Walle, and S. Van Hoecke, "Convolutional neural network based fault detection for rotating machinery," *Journal of Sound and Vibration*, vol. 377, pp. 331–345, 2016.

[17] X. Guo, L. Chen, and C. Shen, "Hierarchical adaptive deep convolution neural network and its application to bearing fault diagnosis," *Measurement*, vol. 93, pp. 490–502, 2016.

[18] M. Xia, T. Li, L. Xu, L. Liu, and C. W. De Silva, "Fault diagnosis for rotating machinery using multiple sensors and convolutional neural networks," *IEEE/ASME transactions on mechatronics*, vol. 23, no. 1, pp. 101–110, 2017.

[19] L. Wen, X. Li, L. Gao, and Y. Zhang, "A new convolutional neural network-based data-driven fault diagnosis method," *IEEE Transactions on Industrial Electronics*, vol. 65, no. 7, pp. 5990–5998, 2017.

Biography

__Anish Gorantiwar__ was born in Ahmednagar, India and received his B.S. degree in Mechanical Engineering from Maharashtra Institute of Technology (MIT). He is currently pursuing his PhD at the Center for Tire Research (CenTiRe) Lab at Virginia Tech with focus in research areas of Dynamics and Control systems.

__Rajvardhan Nalawade__ was born in Ahmednagar, India. He received his B.S. degree in Mechanical Engineering from College of Engineering Pune in 2019. During his undergraduate education, has has been involved in several vehicle dynamics related projects and has been a summer intern at Cummins, Fiat Chrysler and Tata motors. He has three technical publications and a provisional patent in the domain of mechanical engineering. He pursued MS in mechanical engineering at Virginia tech and specialized in estimating vehicle states using intelligent tires.

Arash Nouri *received his PhD in Mechanical Engineering from Virginia Tech. He received his B.Sc. in Aerospace Engineering from K.N.Toosi University of Technology, Iran and later received his M.Sc. in Mechanical Engineering and M.A in Data Analytics and Applied Statistics from Virginia Tech. His expertise is mainly in the fields of autonomous systems, signal processing and statistical learning.*

Vahid Sotoudeh *received his PhD and MS degrees in Civil and Structural Engineering from Stanford University, and his BS in Structural Engineering from University of Illinois Chicago. During his PhD research at Stanford, he studied and developed novel instrumentation and digital signal processing techniques for ambient and strong motion structural vibration measurement and analysis for system identification purposes. He has over 20 years of industry experience at Seismotek, EIP Microwave, DSP Technology and Data Physics.*

Behzad Moslehi *is the CEO/CTO of IFOS. He has extensive knowledge and experience in the development and commercialization of photonic sensing and signal processing systems for monitoring and control of high value assets in demanding environments. He helped to commercialize pioneering fiber optic gyroscopes and sensor arrays at Litton systems. Dr. Moslehi received a PhD and an MS degree in Electrical Engineering and an MS degree in Applied Physics, all from Stanford University. He is a senior member of IEEE, OSA, and SPIE, and a member of SPE.*

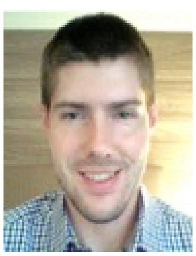

William Price *is the Strategic Programs Manager at IFOS.*

Zahiri Feraidoon *is an engineer at the US Air Force, received his Master of Science degree in Engineering Mechanics from Penn State University. He has more than 20 years of experience in technology research, development, and transition in numerous scientific and engineering disciplines. He has overseen large-scale decision-support projects incorporating analytics, simulation, and visualization for resource allocation, system troubleshooting and repair, and data-driven predictive maintenance. He was selected as a winner of the Small Business Technology Council's (SBTC) 2017 "Champion of Small Business Technology Commercialization" Award, for his role in filling a critical technology gap in the Air Force Sustainment community. He has played a critical role in providing opportunities for small business to promote the technology across all DoD services, boosting their technology transition even further.*

Saied Taheri *is a Professor of Mechanical Engineering at Virginia Polytechnic Institute and State University. He has been the founding director of NSF I/UCRC Center for Tire Research (CenTiRe) since 2012 and the director of Intelligent Transportation Lab since 2008. He has 31 years of academic and industrial experience in automotive engineering, dynamics and control, intelligent systems, wavelets and machine learning with applications in intelligent tires and vehicles, vehicle dynamics and control, automotive and transportation safety and railroads. He has directed 10 post-docs/visiting scholars, 20 doctoral dissertations, and 23 MS thesis. He received his B.S., M.S. and Ph.D. in Mechanical Engineering from Clemson University in 1984, 1986 and 1990, respectively.*